

PAPER • OPEN ACCESS

A New Perspective on Offshore Wind Turbine Certification Using High Performance Computing

To cite this article: Francesco Papi and Alessandro Bianchini 2024 *J. Phys.: Conf. Ser.* **2767** 052008

View the [article online](#) for updates and enhancements.

You may also like

- [Conflicting scientific views on the health risks of low-level ionising radiation](#)
Roger H Clarke
- [SRP Workshop on Exemption and Clearance Levels](#)
- [Meeting report](#)

PRIME
PACIFIC RIM MEETING
ON ELECTROCHEMICAL
AND SOLID STATE SCIENCE

HONOLULU, HI
October 6-11, 2024

Joint International Meeting of
The Electrochemical Society of Japan (ECSJ)
The Korean Electrochemical Society (KECS)
The Electrochemical Society (ECS)

Early Registration Deadline:
September 3, 2024

MAKE YOUR PLANS NOW!

A New Perspective on Offshore Wind Turbine Certification Using High Performance Computing

F. Papi^{1*}, A. Bianchini¹

¹Department of Industrial Engineering, Università degli Studi di Firenze, via di Santa Marta 3, 50138, Florence, Italy

*fr.papi@unifi.it

Abstract. A correct estimation of fatigue and ultimate loads on the structure is key for wind turbine design and certification. In a greater perspective, wind turbines are large structures placed in the natural environment and are thus subject to environmental loads that are stochastic in nature. In the case of offshore turbines, the design space is even vaster, as wind speed, turbulence intensity, wave height and period, and wind/wave direction need to be considered. Due to this complexity, standardization is a challenge, and current design standards prescribe load calculations to be performed on a site-per-site basis. Performing this task requires obtaining a long-term statistical representation of the installation site, which can be complex. Moreover, this process is affected by uncertainties. This work explores an alternative to this approach, i.e., partially, or entirely simulating the lifetime of the offshore asset. Results show how this method can reliably predict fatigue loads even using as little as one year of data. On the other hand, prediction of extreme loads is influenced by the sample size and time-period.

1. Introduction

Effective exploitation of offshore wind energy is key to reach our renewable energy generation targets [1]. To design safer, more reliable, and cheaper offshore wind turbines, design loads need to be accurately estimated. Wind turbine load calculation is a complex topic, as wind turbines operate in the open environment, and are thus subject to stochastic environmental conditions, which determine their loading level [2]. Moreover, the way the turbine and the elements around it, such as the electrical grid, operate, also influences the component's design loads. Onshore wind turbines have benefitted from decades of refinement. International design standards are mature and provide detailed guidelines for their design and load calculation. With respect to offshore turbines, they also operate in a simpler environment, as they are not influenced by sea loads such as waves, currents, and tides. Due largely to the complex environment offshore wind turbines operate in, design guidelines are less mature. In fact, while onshore wind turbines are designed based on a "turbine class" approach, whereby standard environmental conditions are defined by the guidelines, and turbines that meet the guidelines can be installed in sites with corresponding environmental conditions, offshore wind turbine loads need to be computed on a site-per-site basis [3,4]. Designers are thus required to obtain the long-term environmental characteristics of the installation site in terms of the statistical distribution of the main environmental variables.

Such analysis can be complex, as the combination of multiple environmental variables are needed to represent the wind and sea conditions of the site. For fatigue analysis, the design space is generally divided into a series of bins. At least one turbine simulation for each bin is carried out, and the lifetime



fatigue load is derived by summing the loads in all the bins weighed by the probability of each bin. How many and which environmental bins to consider all have an influence on the load estimation and is a topic of active research [5,6].

On the other hand, the computation of environmental contours, defined as the combination of extreme environmental conditions with a certain, rare, probability of occurrence, often needs to be defined for the analysis of extreme loads. This is, similarly to fatigue loads, also complex, as the existing body of scientific literature on the topic demonstrates [7–9]. Moreover, wind turbines in general (especially offshore ones) and particularly floating turbines, are highly non-linear. As such, the extreme loads on a component may not be recorded necessarily during the most severe weather conditions. Therefore, extreme loads occurring during normal operation also need to be computed. A probabilistic approach is generally prescribed for such loads, which are computed based on statistical extrapolation of a limited number of simulations [3]. This is, once again, complex, and, as some authors have demonstrated [10,11], the final load estimation depends on many factors often left for the designer to choose. Based on these premises, this study, inspired by the work of Koo et al. [12], explores a possible alternative load calculation strategy that leverages High Performance Computing (HPC). HPC is used to run hundreds of thousands of simulations of a FOWT, thereby simulating partly or entirely the turbine's life. Fatigue and extreme loads can be computed based on statistical analysis of the simulation outputs. The load estimates are compared to loads computed with a more traditional approach that follows design guidelines indications. Public databases similar to this exist, although examples are scarce. Some of the most notable are the 96-year database computed by Barone et al. [13,14] for an onshore wind turbine, and the work of Graf et al. [6] for a floating turbine. Both the aforementioned databases, however, only include simulations between cut-in and cut-out, and do not include any transient events such as shut-downs or idling in low and high winds.

The study is organized as follows. In section 2 the methods to determine the environmental conditions for the simulations, the wind turbine model, and the methods to compute design loads are presented. In section 3 a selection of results is presented. The two methods are compared in terms of fatigue loads. Extreme loads computed using HPC are also presented, while they are not compared to extreme loads computed with an approach that is truer to standards for reason that will become clear in the following. Finally, some conclusions are drawn, and future outlook is given in section 4.

2. Methods

This study compares two methods for the computation of fatigue and extreme FOWT loads. The first method is based on a statistical analysis of the environmental conditions the FOWT faces. We will refer to this method as *statistics-first*. The second method leverages HPC and is based on statistical analysis of the simulation outputs. We will refer to this method as *loads-first*.

2.1. Environmental conditions

As discussed in section 1, according to current design standards [3,4], offshore wind turbine design is not based on a standardized “class” approach such as those developed for onshore machines [15]. Instead, FOWT designs must be verified in the environmental conditions of the installation site. In this study, the environmental conditions of an offshore site west of the island of Barra (Scotland) have been used. This site was already used in several research projects [16,17], including the FLOATECH project [9,18], to which the authors took part. For brevity, the met-ocean conditions used in this study are only summarized herein. A more complete description can be found in [9]. Met-ocean conditions are specified as a function of four environmental variables: wind speed (U), significant wave height (H_s), peak spectral period (T_p) and wind-wave misalignment (M_{ww}). H_s includes both wind-driven waves and swell, as such, M_{ww} can be significant, especially in case of lower wind speeds, as shown in [9]. Wave direction is determined based on M_{ww} by considering wind direction as constant. Raw data is sourced from the open-access reanalysis database ERA5 [19] and spans a total of 22 years for fatigue analysis (1978 – 2000). For extreme analysis, such a horizon is not enough to obtain the desired 50-year load

and thus the time interval is expanded to 1972-2022, spanning a total of 51 years. This additional data is also sourced from ERA5 [19]. The effects of local orography on the environmental variables, although arguably limited for an offshore installation site, can be included in the long-term reanalysis data if local measurements of wind and waves are available, by means of correlation and correction. This work focuses on the methodology and, also due to lack of local measurements, does not consider such a step; it is postulated however, that this does not affect the generality of the analysis. To have an overview of the scatter plot of Hs as function of U and the environmental contours with return periods of one and fifty years the reader is referred to [9]. To reduce complexity, currents are not included in the present study, although these could influence loading, especially on the mooring lines.

2.1.1. Design space for fatigue loads. Fatigue loads are cyclic in nature and thus depend on the most likely working conditions of the asset. In the *statistics-first* method, the design space is divided in a series of 4-dimensional bins. Three one-hour simulations with three distinct nacelle yaw-errors (0° and $\pm 10^\circ$) are performed within each bin. To reduce the number of bins, two methods first proposed by Stewart [5] are used: the *bin reduction* method, whereby to reduce the number of total environmental bins the width of each bin is increased, and the *probability sorting* method, whereby the least likely bins are not considered in the fatigue analysis. The ranges and widths of the bins determined based on the *bin reduction* method in the four environmental dimensions are specified in Table 1. With these ranges, the number of total bins is found with the *probability sorting* method and depends on what portion of the design space is covered [18]. Both methods trade fatigue load estimation accuracy for reduced computational cost, as explained in [5]. In this study, four levels of total probability coverage are considered, ranging from 95% of the total probability of the considered design space to 80%, as shown in Table 3. In an attempt to better estimate loads on sensors dependent on M_{WW} , an additional set of bins is introduced, “P95 9wb”, where the total probability coverage of 95% is maintained but the M_{WW} bins are increased from six to nine. Despite the increase in M_{WW} bins, this division of the design space results in a reduced number of total bins. This is an interesting consideration and demonstrates that increasing bin size may not always lead to the least number of total bins. The decrease in total bins has also interesting implications on the results and will be discussed in detail in section 3.1. In the *loads-first* method, one simulation for each hour the turbine is installed at the site is performed, using the environmental conditions from the ERA5 database without additional pre-processing. The total number of simulations that are required to compute fatigue loads are shown in Table 2 and depend on the length of the simulated interval. For a fair comparison to the *statistics-first* method, a yaw error of 0° and $\pm 10^\circ$ is selected randomly for each simulation.

Table 1. Bin range and width for statistics-first method.

Parameter	Range	Bin width
U [m/s]	4-26	2
Hs [m]	0-14	2
Tp [s]	3-21	2
M_{WW} [$^\circ$]	-180 – 180	60

Table 2. Simulations for loads-first method.

n° yr.	Λ (cut-in<V<cut-out)	n° sims.
1	0.9045	7929
5	0.9045	39456
10	0.9045	79292
20	0.9045	158584

Table 3. Total probability and number of simulations in statistics-first method.

Probability	Pt	Pt cut-in<V<cut-out	Bin num. cut-in<V<cut-out	Nacelle yaw error	Total simulations
P95 9wb	0.9556	0.9506	302	$0^\circ, \pm 10^\circ$	906
P95	0.9548	0.9500	332	$0^\circ, \pm 10^\circ$	996
P90	0.9077	0.9019	251	$0^\circ, \pm 10^\circ$	753
P85	0.8562	0.8562	197	$0^\circ, \pm 10^\circ$	591
P80	0.8056	0.8218	165	$0^\circ, \pm 10^\circ$	495

2.2. NREL 5MW OC4 FOWT

The load-computation strategies are tested on the NREL 5MW OC4 semi-submersible FOWT, an open-access model defined in [20]. The model makes use of the NREL 5MW RWT rotor [21], representative of a utility-scale multi-MW wind turbine, mounted on the DeepCwind semisubmersible floating platform. The same tower design that was developed for use on the OC3-Hywind spar platform [22] is used. The semi-submersible floater consists of a main central column connected to the tower and three side columns spaced 120° apart. Three 120° catenary mooring lines are used to anchor the turbine to the seabed with one mooring line pointing directly upwind and the other two downwind.

The NREL 5MW OC4 FOWT is simulated in OpenFAST v3.0.0 [23]. Aerodynamics are modelled with Blade Element Momentum theory, augmented with Øye's dynamic induction model [24] and a Beddoes-Leishman type dynamic stall model [25]. Structural dynamics are handled by the ElastoDyn model of OpenFAST and are based on a modal approach. Mooring cables are modelled with a dynamic cable model. Hydrodynamics are included through a potential-flow approach, whereby added mass, damping, and excitation matrices are pre-computed and fed to the OpenFAST model. Viscous drag and damping are included through Morrison's equation. The model has been tested and verified extensively with respect to other state-of-the-art simulation tools [26,27]. Second-order difference and sum-frequency loads however are not included in this study to limit computational time.

2.3. Damage Equivalent Loads

Damage Equivalent Loads (DELs) are used in this study to compare cyclic loading on the various structural components of the turbine. For every simulation, each with a unique combination of environmental conditions, 1-Hz DELs (Eq. 1) are computed using the python toolbox "pyFAST" [28]:

$$DEL = \left(\frac{\sum_{j=1}^{128} n_j S_j^m}{N_{1Hz}} \right)^{1/m} \quad (1)$$

where n_j is the number of load cycles with amplitude S_j recorded in each simulation, m is the Wöhler curve exponent, in this study equal to 4 for steel components and 10 for composite ones, N_{1Hz} is the number of equivalent cycles, equal to the simulation length in seconds, and j is the load bin index. A total of 128 bins are considered in this study. 1-Hz DELs can be aggregated to compute the equivalent load over the entire lifetime of the turbine. For the *loads-first* method, Lifetime DELs are computed as follows:

$$DEL_{life}^{LF} = \frac{T_{life} A}{T_{sym}} \left(\frac{\sum_{i=1}^{A * Nyrs * 8766} T_{eq_i} DEL_i^m}{N_{life}} \right)^{1/m} \quad (2)$$

where T_{sym} is the fraction of lifetime of the turbine that is simulated (e.g. 1, 2, 5 years), $N_{life} = 1E7$ and A is the fraction of time the environmental conditions are within the operating environmental window ($V_{in} < V < V_{out}$). As apparent in Eq. 2, they are simply the weighted sum of the 1Hz DELs in the period considered. On the other hand, lifetime DELs for the *statistics-first* method are the probability-weighted sum over the considered environmental bins and are computed as follows:

$$DEL_{life}^{SF} = \left(\frac{T_{life} \sum_{i=1}^{n_{bins}} p_i T_{eq_i} DEL_i^m}{N_{life} p_t} \right)^{1/m} \quad (3)$$

where p_t is the fraction of total probability between cut-in and cut-out that is accounted for.

2.4. Extreme Loads

Extreme loads on wind turbine components are often defined as extreme loads with a 50-year return period. In international standards, this return period appears often in extreme load calculations. It is used to compute environmental contours, which define the met-ocean conditions used to run ultimate load simulations. Moreover, statistical extrapolation techniques are used to find the extreme loads occurring in normal operation ([15], Annex G). In the *loads-first* method, loads are extracted from each simulation

and collected. They are ordered based on their magnitude and the cumulative probability distribution is computed as:

$$CDF(x_i) = \frac{\sum_i n(x_i)}{N_{tot}} \quad (4)$$

where N_{tot} are the total number of simulations and $n(x_i)$ are the simulations with maximum load x_i . The exceedance probability is computed as the reciprocal of CDF as:

$$EXP(x_i) = 1 - CDF(x_i) \quad (5)$$

The exceedance probability associated with an event of duration τ for a return period of T is computed as:

$$EXP(T) = \frac{\tau}{T} \quad (6)$$

The extreme load associated with a certain return period T is the value of x : $EXP(x) = EXP(T)$.

3. Results

3.1. Statistics

The maximum, minimum, and mean values of key load sensors as recorded during the 50-years of simulation are shown in Fig. 1. Simulations in the operating mean wind speed range are highlighted, as only this portion of the data is used for fatigue analysis. This is done to keep the comparison between the statistics-first and loads-first methods fair, as only fatigue loads between cut-in and cut-out (DLC 1.2 in [15]) are considered in the latter. In addition to being useful for preliminary consistency checks, this data is useful to highlight the differences in the analyzed load sensors and can help explain some of the trends that are observed later in the study.

Past cut-out the turbine shuts down and aerodynamic loads decrease, as demonstrated by the lower upwind mooring tension, blade root out-of-plane bending moment (BR_1 Myc), and tower base fore-aft moment (TB My, Fig. 1 (a,b,c)). Moreover, BR_1 Myc, and TB My show strong dependence on aerodynamic loads, as, similarly to aerodynamic thrust, they peak around the rated wind speed. Mooring line 2 fairlead tension (T_{ML2}), on the other hand, despite being influenced by aerodynamic loading, appears to also be influenced by other environmental variables as minimum and maximums do not follow this trend.

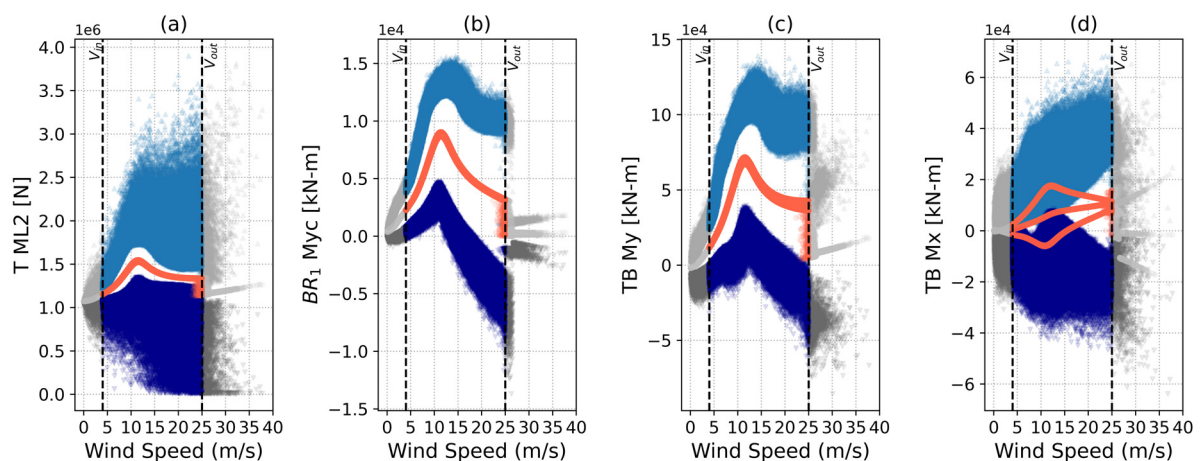


Figure 1. Scatter plots of various quantities as a function of mean wind speed. Means (red), maximums (light blue) and minimums (dark blue). (a) Fairlead tension of upwind mooring line, (b) out-of-plane blade root bending moment, (c) fore-aft tower base bending moment, (d) side-side tower base bending moment. Results in section 3.2 (fatigue loads) are based on colored data between cut-in (V_{in}) and cut-out (V_{out}), data beyond operating range in grey, used in section 3.3 for extreme loads.

Side-side tower base bending moment (Fig. 1 (d)) is similar in this regard and maximum and minimum loads increase monotonically as wind speed increases. For this load sensor, mean loads show strong dependence on nacelle yaw error, which is the cause for the three distinct mean trends in Fig. 1 (d).

3.2. Fatigue loads

For fatigue loads, a 22-year subset, from 1981 to 2000, of the 51 years of simulated data is used. This was done to keep the comparison to the *statistics-first* method rigorous as this 22-year subset of data was used to compute the probability of the wind speed bins in Tables 1 and 3, as detailed in [9]. Fatigue loads in the form of 20-year Lifetime DELs recorded during normal operation are shown in Fig. 2 (a-d) for key load sensors on the turbine structure.

For the *loads-first* method, lifetime DELs obtained with subsets of the 22-year dataset of different lengths are compared. Operating points where the wind speed is below cut-in or above cut-out, i.e., where the turbine is parked or idling, were removed from the samples. The sample size is computed as $n_{yrs} * A * hrs_{yr}$, with A being the fraction of time the wind speed is between cut-in and cut-out, computed based on the entire 22-year dataset. For each interval, the ninety-percent confidence intervals, shown as whiskers in Figs. 2, are computed as the 5th and 95th percentiles of two-thousand

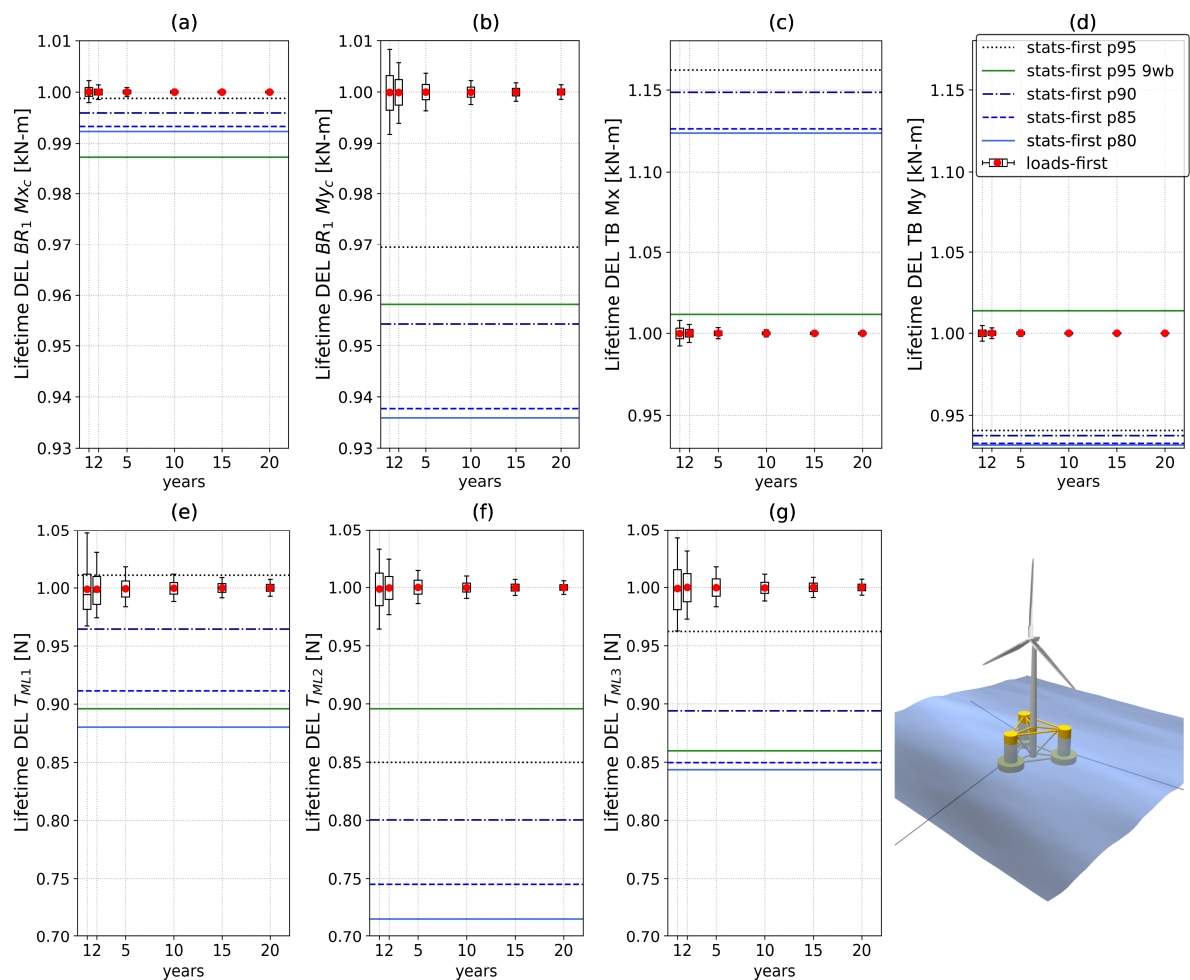


Figure 2. Lifetime DELs on selection of load sensors for statistics-first method as a function of simulated time. For each interval, red dot represents median, solid dash mean value, boxes are the first and third quartiles and whiskers are 5th and 95th percentiles of 2000 bootstrap samples of 22-year data. Lines represent value obtained with loads-first method with bin combinations in Table 3.

bootstrapped samples of the 22-year data. The two-thousand samples are extracted randomly from the data using a uniform probability density function (PDF). Through bootstrapping of the statistics, the year-to-year variability is effectively removed from the analysis. As such, the whiskers in Fig. 2 indicate the result that is obtained nine times out of ten when computing fatigue loads based on a random subsample of the 22-year data. It must be noted that the influence of year-to-year variability is a potential drawback of the loads-first method that we plan to investigate in future studies. The bootstrapped Lifetime DELs are compared to estimates using the bin reduction and sorting techniques, considering different levels of total coverage of the probability space as described in section 2. All the results are normalized with respect to the median value of the 2000 bootstrap samples with 20-year length, which is assumed as reference.

As shown in Fig. 2, the 20-year sample-to-sample variability is very small, indicating that lifetime DELs can be reliably estimated with 20-years of data. Decreasing the amount of data in the samples, the 90% confidence interval widens but remains smaller than 2% for all sensors in the case that only one year of data is considered. If this result, obtained with the *loads-first* approach is compared with the *statistics-first* approach, good agreement can be noted between the two, despite the drastically different number of simulations and computational time required in the *statistics-first* approach. Larger differences, on the order of 15% for side-side and 5% for fore-aft loads can be noted in the case of tower base bending moments. As shown in Fig. 2, however, this difference can be drastically reduced if a different binning strategy is used for M_{WW} . While this binning strategy is an improvement for tower base DELs, if blade root loads are concerned, P95 predictions using nine M_{WW} bins are farther from the 20-year median than P95 with six M_{WW} bins. The reasons for this different agreement between the two methods will be explained in more detail in the following sections.

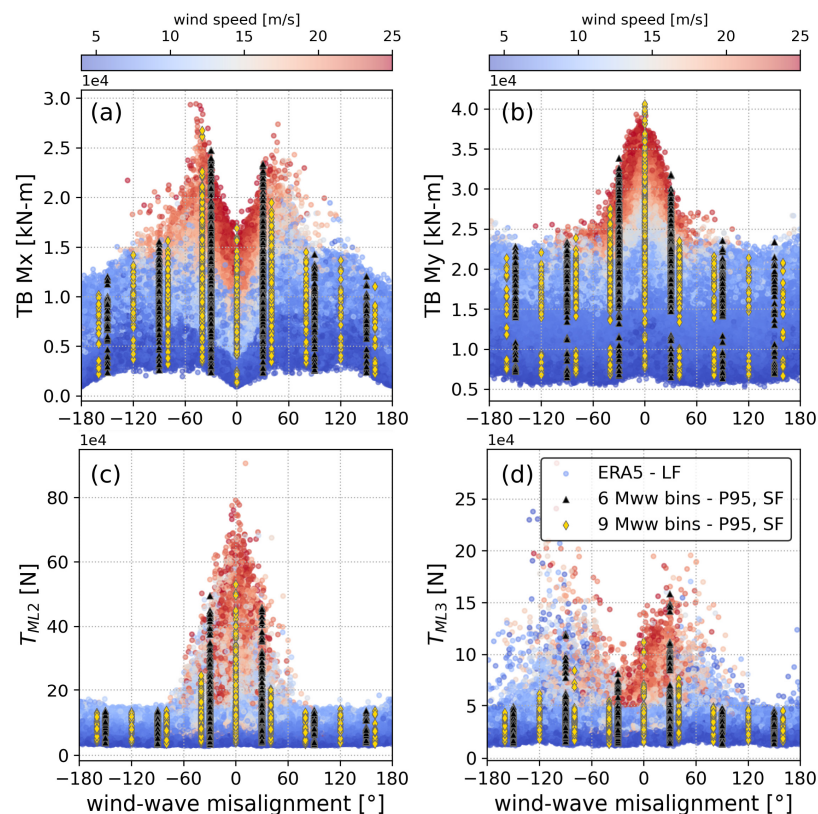


Figure 3. 1-Hz DELs as a function of M_{WW} for key load sensors in simulations used is statistics-first (SF) and loads-first (LF) methods. DELs are colored cool to warm as a function of mean wind speed. Simulations outside of the cut-in – cut-out range are excluded. In black and in yellow data computed for statistics-first method with P95 (6 Mww bins) and P95 9wb (9 Mww bins) – Table 3.

Lifetime DELs recorded at the fairleads of the mooring lines are shown in Fig. 2 (e-g). Despite the larger 90% confidence intervals, fatigue loads computed with 20 years of data are largely insensitive to variations in the data sample and represent a good estimate of Lifetime DELs. When one year of data is considered, 90% confidence interval widens to 7-8% of the 20-year median. Despite the increased uncertainty, the *loads-first* approach still outperforms the *statistics-first* method regardless of the total probability that is considered, except for the tension on the first fairlead. This is somewhat to be expected because one year of data in the *loads-first* method means using eight to ten more times the simulations (7929 versus 996 for P95).

The increased computational time can be however outweighed by the decreased pre-processing burden in the *loads-first* method. Moreover, contrary to tower base lifetime DELs, switching to nine M_{WW} bins only improves agreement with respect to the upwind fairlead tension (T_{ML2}). The influence of M_{WW} binning can be explained by observing Fig. 3, where scatter plots of 1Hz DELs recorded during the 22 simulated years are shown compared to those computed in the *statistics-first* methods with both five and nine M_{WW} bins. As shown by the colorbar in Fig. 3, as the wind speed increases, the spread in M_{WW} decreases, indicating that waves are increasingly wind-driven. The data points computed with nine M_{WW} bins are able to better capture the distribution of the 22-year data points, especially around 0° M_{WW} , for both side-side and fore-aft tower base bending moments and for mooring line tension at fairlead 2. However, this is not the case for fairlead 3, where high tension data points in the -120° to -60° and 30° to 100° M_{WW} range are not properly captured using nine M_{WW} bins.

3.3. Extreme loads

The extreme load wind turbine components are required to resist is often defined as the extreme load with a 50-year return period. The exceedance probability of a selection of load sensors on the 5MW FOWT are shown in Fig. 4. Exceedance probability is computed using Eq. (6) for various consecutive samples of 1-, 5- and 20-year lengths. The one computed using the full 50 years of data is shown in black. The 50-year extreme load is the intersection between the exceedance probability curve and the 50-year exceedance probability line. When a sample size smaller than 50 years is used, statistical extrapolation is required to extrapolate the loads to the 50-year exceedance probability, whereby a continuous CDF is fit to the data and used to extrapolate the extreme load with the required return period. No such technique is applied in this study, where focus is put on sample size and sample-to-sample variability instead. Both at tower base and at blade root, in-plane loads such as TB M_x and $BR_1 M_{xc}$ show more sample-to-sample variation than out-of-plane loads such as TB M_y and $BR_1 M_{yc}$. As shown in Fig. 1, the latter are mostly influenced by aerodynamics, while other environmental variables such as H_s and M_{WW} have non-negligible influence on the former. As such, extreme events are more spread out for side-side loads, as demonstrated by the shape of the exceedance probability curves in Fig. 4 (a, c), that decrease more gradually than out-of-plane loads (Fig. 4 (b, d)). Therefore, the difference in the predicted on-year extreme load using one year of data for TB M_x (Fig. 4 (a)) can vary up to 25%. On the other hand, out-of-plane loads show less sample-to-sample variation and the estimates of the exceedance probability curve computed using twenty years of data agree well with the fifty-year reference. Mooring line tensions (Fig. 4 (e,f)) show even greater variability than in-plane loads. Extreme events are much more scattered and sample-to-sample variability is very pronounced. In fact, if we analyse the exceedance probability computed with one year of data in Fig. 4 (f), the difference between the greatest and smallest one-year extreme load is approximately 40%. Focusing on the upwind mooring line, which is the most loaded (Fig. 4 (e)), the difference between the greatest and smallest one-year extreme load is approximately 37.5%. If 5-year extreme loads are considered the variability is 23.5% and if 20 years are considered it is reduced to a still considerable 5.8%. This difference is still relevant because it is expected to increase if the 20-year trends are extrapolated to 50 years through statistical fitting and extrapolation. This uncertainty needs to be compared to that of the *statistics-first* method, which will be the topic of a subsequent study.

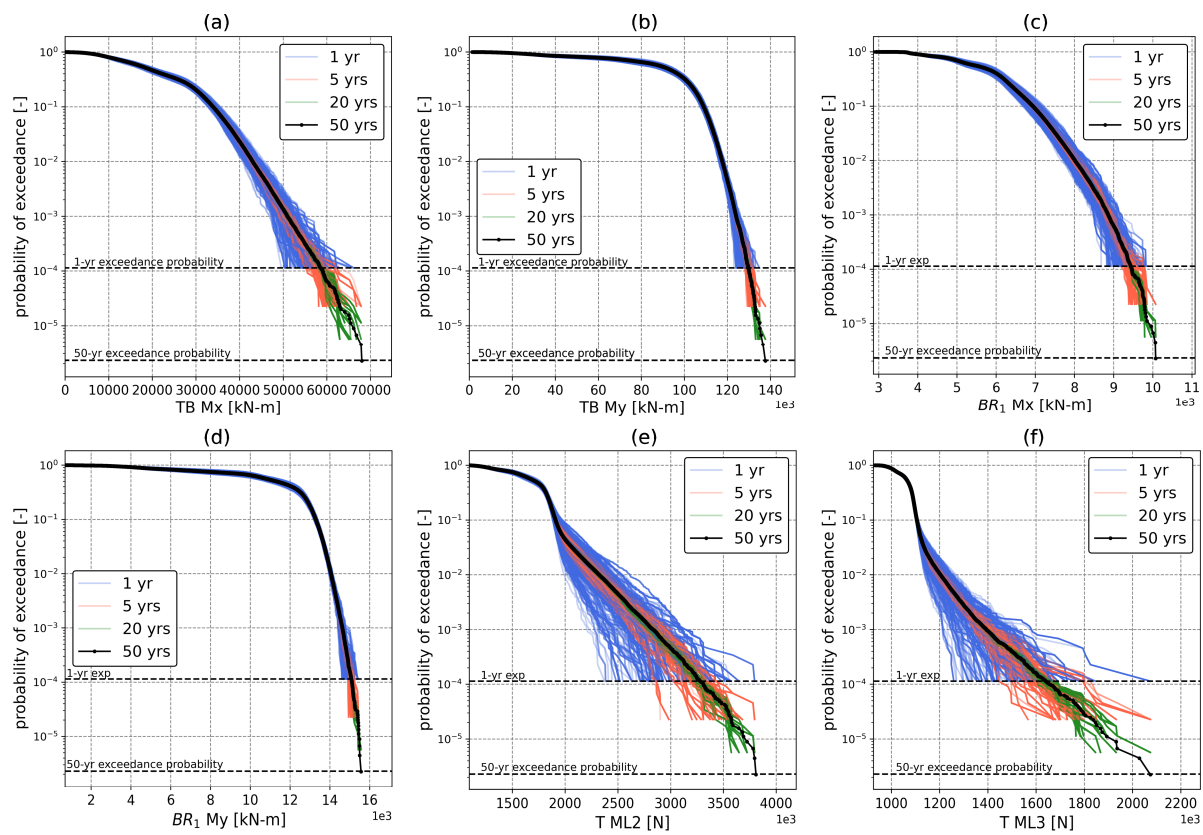


Figure 4. Exceedance probability for key load sensors computed with 500 random subsets of consecutive data for each interval length. Tower base side-side bending moment (TB Mx, a), fore-aft tower base bending moment (TB My, b), in-plane (BR1 Mx, c) and out-of-plane (BR1 My, d) blade root bending moment, and fairlead tension of mooring lines #2 and #3 (T ML2,3, e,f).

4. Conclusions

In this study the alternative “loads-first” method, which leverages HPC for the computation of extreme and fatigue FOWT loads, is proposed, and critically analysed. Fifty years of simulation of the NREL 5MW OC4 reference design are used to compute fatigue and extreme loads. The robustness of the method is evaluated by varying the sample size used to compute the loads, i.e., by subsampling the 50-year dataset and through statistical techniques such as bootstrapping.

If fatigue loads are concerned, this research suggest that reliable estimations of the lifetime DELs of various key load sensors can be obtained using as little as 1 year of data. It must be noted that this still involves running thousands of 1-hour simulations. However, no statistical analysis of the site is required, shortening set-up time. Before these results can be generally applied, however, it must be noted that the bootstrapping method used to evaluate sample-to-sample variation of fatigue load prediction partially compensates for year-to-year variability in environmental conditions, which needs to be accounted for. If the mean value of the 20-year bootstrapped data is assumed as reference, the *loads-first* method performed better than the *statistics-first* counterpart (at the basis of current standards’ prescriptions) in terms of lifetime DEL prediction for most load sensors, most notably mooring line tensions. While the *statistics-first* method requires much fewer simulations and could be refined to better predict fatigue loads on the FOWT by increasing the number of environmental conditions that are evaluated, the results of this study show the importance of number and choice of environmental bins in lifetime DELs. As for extreme loads, exceedance probability of key load sensors computed with consecutive subsets of the fifty years of data of different lengths are critically compared. Differently from fatigue loads, the sample size significantly influences extreme load predictions for some load sensors. Similarly to fatigue loads, mooring line tensions show the greatest sample-to-sample variability, which requires a large number of

simulations to reduce. This proves that estimating 50-year extreme loads is challenging even with such a large number of simulations.

An additional outcome of this study is the 50-year dataset of post-processed simulation results, which can act as reference for future studies on the topic of FOWT load calculation.

Overall, the method has shown potential, but also some limitations, particularly in extreme load estimation. These limitations, however, need to be weighed against those of traditional extreme load extrapolation techniques, which are also affected by uncertainty as discussed in the paper. Work on the topic is ongoing and future studies will expand and fine-tune the approach.

Data Availability

The post-processed dataset containing statistics (mean, min., max., standard-deviation, skewness, kurtosis) and 1Hz DELs for each simulation can be found at: <https://zenodo.org/records/10514143>

References

- [1] European Commission 2020 *An EU Strategy to harness the potential of offshore renewable energy for a climate neutral future* (Brussels)
- [2] Veers P, et al., 2023 *Wind Energ. Sci.* **8**, 1071–1131
- [3] IEC 2019 TS 61400-3-1, Wind energy generation systems - Part 3-1: Design requirements for fixed offshore wind turbines
- [4] DNVGL 2018 *DNVGL-ST-0119 - Floating wind turbine structures* (DNVGL AS)
- [5] Stewart G M 2016 Design Load Analysis of Two Floating Offshore Wind Turbine Concepts, PhD Thesis (University of Massachusetts Amherst)
- [6] Graf P A, et al. 2016 *Wind Energy* **19** 861–72
- [7] Haselsteiner A F, et al. 2020 Global Hierarchical Models for Wind and Wave Contours: Physical Interpretations of the Dependence Functions *Volume 2A: Structures, Safety, and Reliability* 39th International Conference on Ocean, Offshore and Arctic Engineering (Virtual, Online: ASME)
- [8] Haselsteiner A F, et al. 2021 *Ocean Eng.* **236** 109504
- [9] Papi F, Perignon Y and Bianchini A 2022 *J. Phys. Conf. Ser.* **2385** 012117
- [10] Schinas P N, et al. 2021 *Wind Eng.* **45** 921–38
- [11] Zhang X and Dimitrov N 2023 *Wind Energy Sci.* **8** 1613–23
- [12] Koo B J, et al. 2022 Life Cycle Response Analysis of a Floating Offshore Wind Turbine, *Presented at 41st International Conference on Offshore Mechanics and Arctic Engineering* (Hamburg, Germany)
- [13] Barone M, et al. 2012 Decades of Wind Turbine Load Simulation *50th AIAA Aerospace Sciences Meeting including the New Horizons Forum and Aerospace Exposition* (Nashville, Tennessee: AIAA)
- [14] Barone M et al. 2012 Simulating the Entire Life of an Offshore Wind Turbine, *Technical Report*
- [15] IEC 2019 TS 61400-1, Wind energy generation systems - Part 1: Design requirements
- [16] Antonia Krieger, et al. 2015 D7.2 LIFEs50+ Design Basis, *Technical Report*
- [17] Vigara F, et al. 2020 COREWIND D1.2 Design Basis, *Technical Report*
- [18] Papi F and Bianchini A 2023 Annotated Guidelines for the Simulation of Floating Offshore Wind Turbines in a Real Environment, *Volume I: Offshore technology*, 42nd International Conference on Offshore Mechanics and Arctic Engineering, V001T01A005 (Melbourne, Australia: ASME)
- [19] Hersbach H, et al. 2020 The ERA5 global reanalysis *Q. J. R. Meteorol. Soc.* **146** 1999–2049
- [20] Robertson A, et al. 2014 *Definition of the Semisubmersible Floating System for Phase II of OC4*
- [21] Jonkman J, et al. 2009 Definition of a 5-MW Reference Wind Turbine for Offshore System Development, *Technical Report*
- [22] Jonkman J 2010 Definition of the Floating System for Phase IV of OC3, *Technical Report*
- [23] National Renewable Energy Laboratory OpenFAST *GitHub*
- [24] Branlard E et al. 2022 *J. Phys. Conf. Ser.* **2265** 032044
- [25] Damiani R R and Hayman G 2019 *The Unsteady Aerodynamics Module for FAST8*
- [26] Papi F et al. 2024 Quantifying the Impact of Modeling Fidelity on Different Substructure Concepts - Part II: Code-to-Code Comparison in Realistic Environmental Conditions, *Wind Energ. Sci.* **9**
- [27] Behrens De Luna R et al. 2024, *Wind Energ. Sci.* **9**, 623–649
- [28] Branlard E Release v3.4.0 · OpenFAST/python-toolbox · GitHub